Journal of the European Ceramic Society 19 (1999) 2757–2762

PII: S0955-2219(99)00077-1
0955-2219/99/$ - see front matter

Oxidation Behavior of Hot-pressed Si_3N_4 with Re_2O_3 (Re = Y, Yb, Er, La)

Heon-Jin Choi,[a]* June-Gunn Lee[a] and Young-Wook Kim[b]

[a]Multifunctional Ceramics Research Center, Korea Institute of Science and Technology, Seoul 130-650, South Korea
[b]Department of Materials Science and Engineering, The University of Seoul, Seoul 130-743, South Korea

(Received 31 December 1998; accepted 13 March 1999)

Abstract

Four different β-Si_3N_4 ceramics with silicon oxynitrides [$Y_{10}(SiO_4)_6N_2$, $Yb_4Si_2N_2O_7$, $Er_2Si_3N_4O_3$, and $La_{10}(SiO_4)_6N_2$, respectively] as secondary phases have been fabricated by hot-pressing the Si_3N_4–$Re_4Si_2N_2O_7$ (Re = Y, Yb, Er, and La) compositions at 1820°C for 2 h under a pressure of 25 MPa. The oxidation behavior of the hot-pressed ceramics was characterized and compared with that of the ceramics fabricated from Si_3N_4–$Re_2Si_2O_7$ compositions. All Si_3N_4 ceramics investigated herein showed a parabolic weight gain with oxidation time at 1400°C and the oxidation products of the ceramics were SiO_2 and $Re_2Si_2O_7$. The Si_3N_4–$Re_4Si_2N_2O_7$ compositions showed inferior oxidation resistance to those from Si_3N_4–$Re_2Si_2O_7$ compositions, owing to the incompatibility of the secondary phases of those ceramics with SiO_2, the oxidation product of Si_3N_4. Si_3N_4 ceramics from a Si_3N_4–$Er_4Si_2N_2O_7$ composition showed the best oxidation resistance of 0·198 mg cm^{-2} after oxidation at 1400°C for 192 h in air among the compositions investigated herein.

Keywords: hot pressing, Si_3N_4, oxidation, corrosion, rare-earth oxides.

1 Introduction

Many properties of Si_3N_4 ceramics are degraded at high temperatures due to the residual grain boundary glassy phase[1,2] that is inevitably present in liquid-phase sintered Si_3N_4. Several attempts to optimize high temperature properties have been investigated, including the crystallization of the amorphous grain boundary phase by a post-sintering heat treatment,[3] the formation of a transient liquid phase,[4] and the reduction of the overall additive content in combination with the use of refractive additives.[5,6]

Work performed by Lange *et al.*[7] on the Si_3N_4–SiO_2–Y_2O_3 system has shown that the high temperature properties of Si_3N_4 can be improved by choosing compositions in the Si_3N_4–Si_2N_2O–$Y_2Si_2O_7$ compatibility triangle, since the Si_2N_2O and $Y_2Si_2O_7$ phases are in equilibrium with SiO_2 (the oxidation product of Si_3N_4). Lange[8] also proposed similar behavior for compositions in the Si_3N_4–SiO_2–CeO_2 system. On this basis, various rare-earth oxides have been studied as potential sintering additives, since it is expected that Si_3N_4–SiO_2–rare-earth oxide systems would also exhibit this type of behavior. It has been shown that rare-earth oxides are as effective as Y_2O_3 in the densification of Si_3N_4.[3,9,10] Furthermore, refractory disilicate, $Re_2Si_2O_7$ (Re refers to the cation of a rare-earth oxide), can be crystallized at grain boundaries, thereby resulting in improved high temperature properties.[3,11–13] These results make the Si_3N_4–$Re_2Si_2O_7$ compositions attractive for the high temperature applications of Si_3N_4.

Recently, a Si_3N_4–$Yb_4Si_2N_2O_7$ composition has also been investigated due to the superior high temperature stability (i.e. high melting temperature) of the $Yb_4Si_2N_2O_7$ phase.[14] As expected, the ceramics showed superior high temperature strength to that of Si_3N_4 from the Si_3N_4–$Yb_2Si_2O_7$ composition.[15] Other rare-earth oxides would have similar phase relationships with that of Si_3N_4–SiO_2–Yb_2O_3 system[3,7,8,16,17] and, therefore, the Si_3N_4–$Re_4Si_2N_2O_7$ compositions could be considered as candidates for high temperature application of Si_3N_4.

In this study, the oxidation behavior of four different Si_3N_4 ceramics prepared from the Si_3N_4–$Re_4Si_2N_2O_7$ (Re = Y, Yb, Er, and La) compositions by hot-pressing was characterized and compared with that of Si_3N_4 prepared from the Si_3N_4–$Re_2Si_2O_7$ compositions.

* To whom correspondence should be addressed. Fax: +82-2-958-5509; e-mail: hjchoi@kistmail.kist.re.kr

2 Experimental Procedure

Commercially available Si_3N_4 (SN E-10, Ube Industries, Tokyo, Japan), Y_2O_3, Yb_2O_3, Er_2O_3, La_2O_3 (99.9%, Johnson Matthey, Seabrook, NH), and SiO_2 (99.9%, Aerosil 200, Degussa Co., NJ) powders were used as starting materials. Four different mixtures corresponding to the Si_3N_4–$Re_4Si_2N_2O_7$ composition were prepared. The total amount of the sintering additives was fixed at 12 vol%. The mixtures were milled in methanol for 24 h using Si_3N_4 balls. The milled slurry was dried, sieved, and hot-pressed at 1820°C for 2 h under a pressure of 25 MPa in a nitrogen atmosphere.

Densities of hot-pressed specimens (designated as SNRe) were measured using the Archimedes method. The theoretical densities of the specimens were calculated according to the rule of mixtures. X-ray diffractometry (XRD) was used to determine the crystalline phases. The hot-pressed specimens were cut, polished, and then plasma-etched by CF_4 containing 7·8% O_2. The microstructures were observed by scanning electron microscopy (SEM). To test for oxidation resistance 18×18×2·5 mm specimens were cut and polished, placed on platinum wire in a box furnace, heated to 1400°C at a heating rate of 450°C h^{-1}, and held at the temperature for 192 h. The furnace was cooled at time intervals of 12–72 h in order to measure weight changes of the specimens. The materials were characterized by XRD to identify crystalline phases present on the surface of the oxidized ceramics. The oxidized surfaces were characterized by SEM and energy-dispersive X-ray spectroscopy (EDX).

3 Results and Discussion

The relative densities of the SNRe are listed in Table 1. The relative densities of ≥98.6% were achieved by hot-pressing with a holding time of 2 h at 1820°C. The highest density was obtained for SNY and the lowest density of 98.6% for SNYb. XRD of the specimens (SNRe) showed β-Si_3N_4 as the major phase and various Re-silicon oxynitrides, $Y_{10}(SiO_4)_6N_2$, $Yb_4Si_2N_2O_7$, $Er_2Si_3N_4O_3$, and $La_{10}(SiO_4)_6N_2$, respectively, as the minor phases (Fig. 1). It is well known that $Y_4Si_2N_2O_7$ phase cannot coexist with Si_3N_4,[7] and, therefore, $Y_{10}(SiO_4)_6N_2$ phase was crystallized for SNY. On the other hand, as reported in a previous study,[15] the $Yb_4Si_2N_2O_7$ phase was easily crystallized for SNYb. Although it is expected that rare-earth oxides would have similar phase relationships with the Si_3N_4–SiO_2–Yb_2O_3 system, $Er_4Si_2N_2O_7$ and $La_4Si_2N_2O_7$ phases were not crystallized for SNEr and SNLa, respectively.

As shown in Fig. 2, the microstructures of SNRe were similar with each other except SNLa, which showed a finer microstructure than the others. It has been reported that the growth rate of the prismatic plane of Si_3N_4 grains in a glass containing rare-earth oxides decreases with increasing the cationic radius of the rare-earth oxide due to the higher degree of the adsorption of cations on the surface of Si_3N_4 grains.[18] Adsorption of cations on the surface of Si_3N_4 grains restricts the adsorption of Si^{+4} and N^{-3} from the glass phase. The cationic radius of La^{+3} ($1{\cdot}160\times10^{-1}$ nm) is larger than those of Y^{+3} ($1{\cdot}011\times10^{-1}$ nm), Yb^{+3} ($0{\cdot}985\times10^{-1}$ nm), and Er^{+3} ($1{\cdot}004\times10^{-1}$ nm). Therefore, the high degree of adsorption of La^{3+} ion on the surface of Si_3N_4 grains may result in the finer microstructure for SNLa.

Figure. 3 shows the relation between the square of the weight gain and the oxidation time at 1400°C. The oxidation behavior of SNRe follows a parabolic rate law of the type;

$$W^2 = kt \tag{1}$$

where W is the weight gain per unit surface area, k is the rate constant of parabolic oxidation, and t is the exposure time. It has been proposed that the parabolic oxidation behavior of Si_3N_4 ceramics indicates that the rate-determining step is a diffusional process associated with the migration of additive cations and anions along the grain boundary phases to the interface between the ceramic and the surface oxide.[2,12] The fast oxidation rate of SNYb and SNLa in the initial stage of oxidation (< 12 h) may be due to the open porosity of the specimens, which showed relatively low densities. The observed weight gains of SNRe after oxidation at 1400°C for 192 h and the rate constants of parabolic

Table 1. Relative density, weight gain, and rate constant (k) of parabolic oxidation for SNRe. For comparison, relative density, weight gain and rate constant of the Si_3N_4 fabricated from Si_3N_4–$Re_2S_2O_7$ compositions[19] were included

	Si_3N_4-$Re_4Si_2N_2O_7$				*Si_3N_4–$Re_2Si_2O_7$*			
	Y	*Yb*	*Er*	*La*	*Y*	*Yb*	*Er*	*La*
Relative density (%)	99·9	98·6	99·1	98·7	99·7	99·9	97·7	98·5
Weight gain (1400°C, air, 192 h, mg cm^{-2})	0·471	0·635	0·375	0·856	0·280	0·413	0·134	0·305
k [$mg^2/(cm^4\times h)\times10^{-4}$]	11·2	12·5	6·0	36·2	3·9	8·1	1·0	4·8

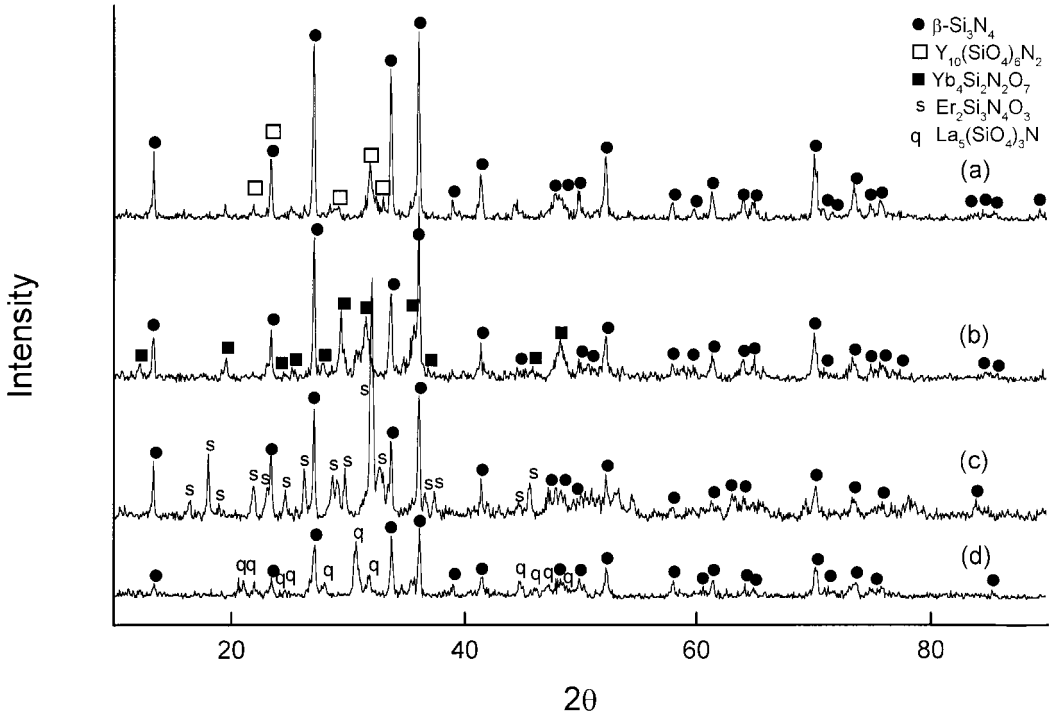

Fig. 1. XRD patterns of SNRe: (a) SNY, (b) SNYb, (c) SNEr, and (d) SNLa.

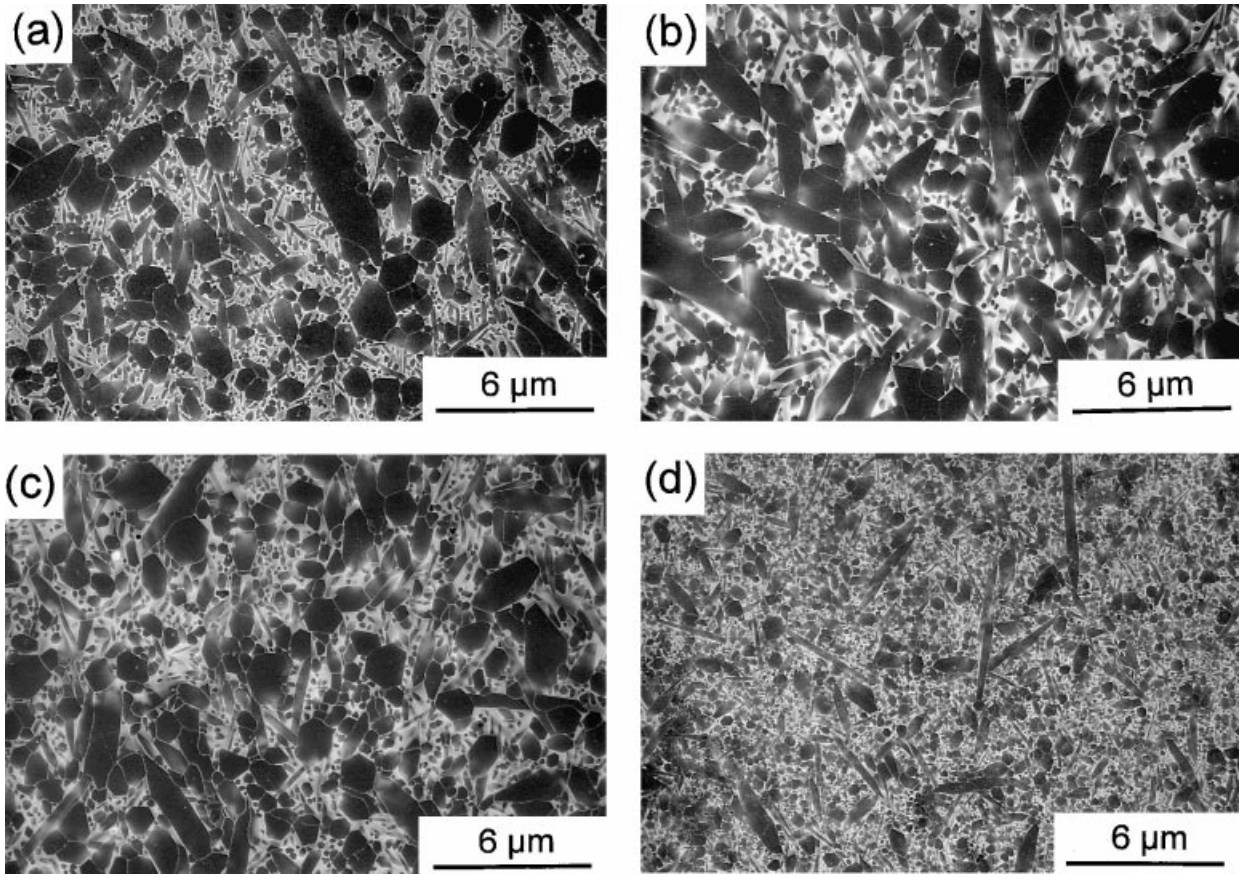

Fig. 2. Microstructures of SNRe: (a) SNY, (b) SNYb, (c) SNEr, and (d) SNLa.

oxidation, k, are listed in Table 1. For comparison, the relative densities, weight gains and rate constants of Si_3N_4 ceramics fabricated from Si_3N_4–$Re_2Si_2O_7$ compositions by hot-pressing under the same conditions[19] are included. The results shown in Table 1 indicate that the oxidation resistance of SNEr, SNY, and SNYb is better than that of SNLa. A refractory nature of grain boundary glassy phase mainly determines the diffusion rate of cations and anions along the residual grain boundary glassy phases and, therefore, the oxidation resistance of Si_3N_4. A greater refractory nature of

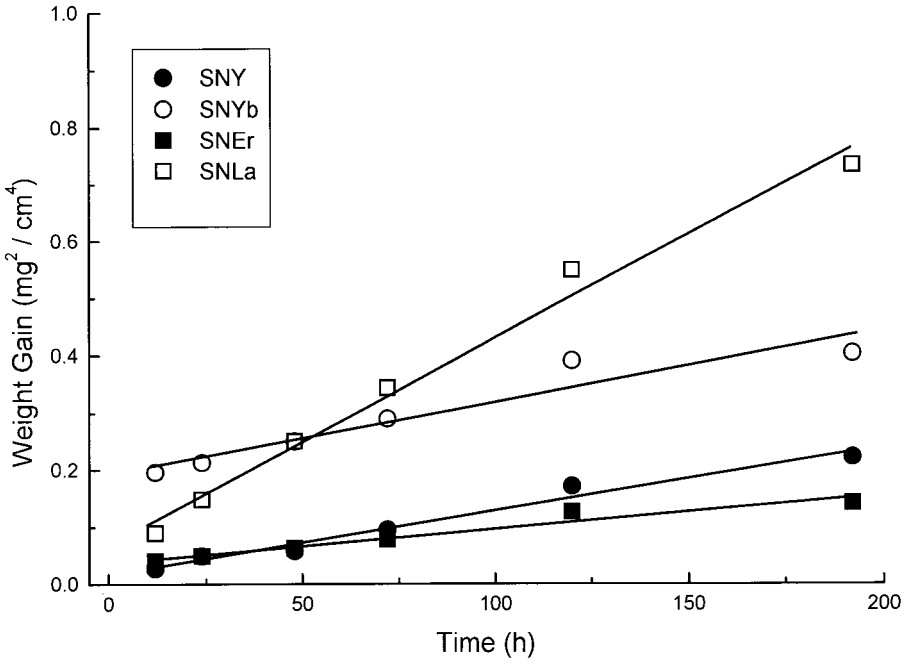

Fig. 3. Parabolic plot of specific weight gains as a function of time at 1400°C.

grain boundary glassy phases is expected for Si_3N_4 sintered with the rare-earth oxide having a smaller cationic radius, e.g. Er_2O_3, Yb_2O_3, and Y_2O_3, due to their strong field strength between cations and anions.[19] Furthermore, it has been reported that the oxidation resistance of Si_3N_4 with rare-earth oxide as sintering additives is reasonably correlated with the eutectic temperature of the rare-earth oxide–SiO_2 system.[12] The eutectic temperatures of the Er_2O_3–SiO_2 system (1680°C), the Y_2O_3–SiO_2 system (1660°C), and the Yb_2O_3–SiO_2 system (1650°C) are higher than that of the La_2O_3–SiO_2 system (1625°C).

The results of this and previous studies[12,19,20] showed that Si_3N_4 sintered with Er_2O_3 showed the best oxidation resistance among the compositions investigated herein. The contribution of the both small cationic radius of Er^{+3} ion and the high eutectic temperature of Er_2O_3–SiO_2 system to the refractoriness of the grain boundary glassy phase can explain the superior oxidation resistance of the ceramics, indicating that Er_2O_3 is a suitable sintering additive for oxidation-resistant Si_3N_4 ceramics.

As shown in Table 1, SNRe fabricated from the Si_3N_4–$Re_4Si_2N_2O_7$ compositions shows inferior oxidation resistance to the Si_3N_4 from Si_3N_4–$Re_2Si_2O_7$ compositions. Figure 4 shows the SEM and EDX image of oxidized surface of SNYb, as a typical example of SNRe. Figure 4(b) indicates that the oxide on the surface contains Yb. XRD of the oxidized surfaces of SNRe only show $Re_2Si_2O_7$ and SiO_2 (Fig. 5).

It has been reported that $Y_{10}(SiO_4)_6N_2$ phase is incompatible with SiO_2 and unstable in an oxidizing condition.[7] It has also been reported that the

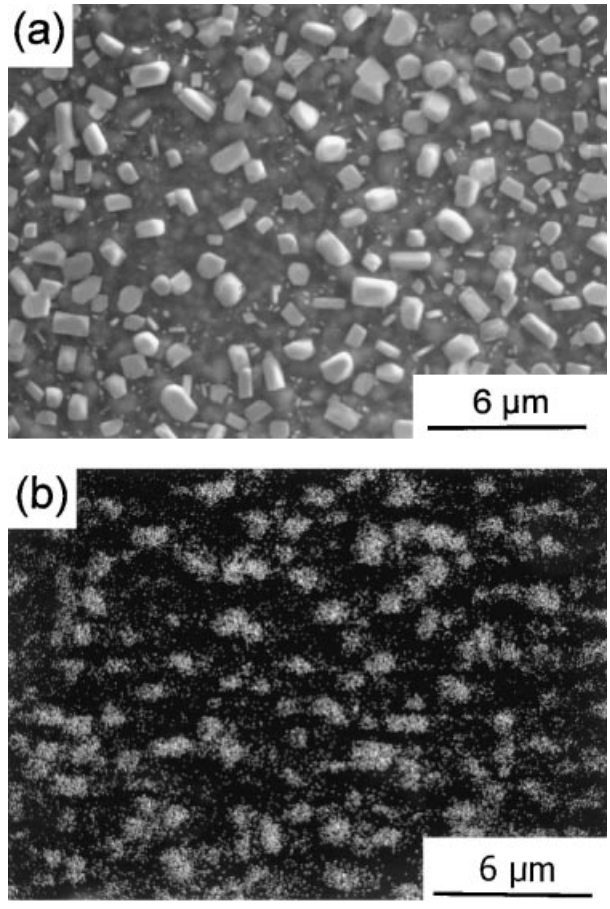

Fig. 4. SEM micrograph of the (a) oxidized surface of SNYb and (b) Yb mapping of the surface.

Si_3N_4 containing $Yb_4Si_2N_2O_7$ is oxidized to form SiO_2 and $Yb_2Si_2O_7$ by the following reactions:[14,21]

$$Si_3N_4(s) + 3O_2(g) = 3SiO_2(s) + 2N_2(g) \quad (2)$$

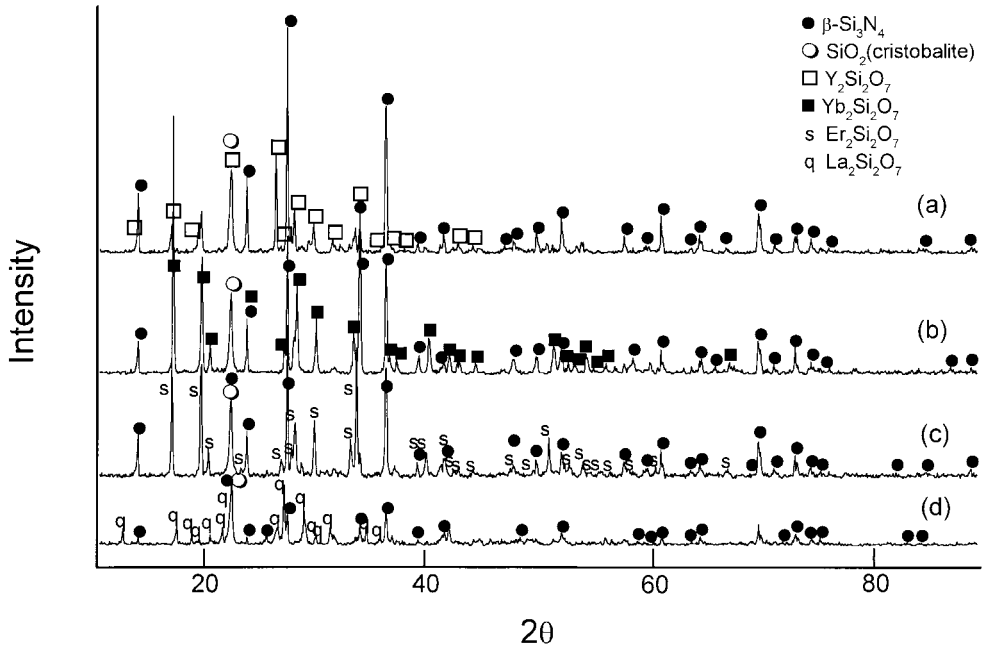

Fig. 5. XRD patterns of the oxidized surfaces of SNRe: (a) SNY, (b) SNYb, (c) SNEr, and (d) SNLa.

$$Yb_4Si_2N_2O_7(s) + 1{\cdot}5O_2(g) = 2Yb_2SiO_5(s) + N_2(g) \quad (3)$$

$$Yb_2SiO_5(s) + SiO_2(s) = Yb_2Si_2O_7(s) \quad (4)$$

Reactions (3) and (4) occur due to the incompatibility of $Yb_4Si_2N_2O_7$ and Yb_2SiO_5 phases with SiO_2 and induce migration of Yb^{+3} ions from the bulk to the oxidized surface. It means that the reactions (3) and (4) enhance the oxidation of Si_3N_4 ceramics. The properties of $Er_2Si_3N_4O_3$ and $La_{10}(SiO_4)_6N_2$ phases have not been clearly identified. However, from the facts that (1) $Y_2Si_3N_4O_3$ and $Y_{10}(SiO_4)_6N_2$ phases are incompatible with SiO_2 and unstable in an oxidizing condition[7] and (2) the oxidation products of Si_3N_4 ceramics containing $Er_2Si_3N_4O_3$ or $La_{10}(SiO_4)_6N_2$ phase are $Re_2Si_2O_7$ and SiO_2, $Er_2Si_3N_4O_3$ and $La_{10}(SiO_4)_6N_2$ phases are expected to be incompatible with SiO_2 and unstable under oxidizing conditions. The $Re_2Si_2O_7$ is also an oxidation product of Si_3N_4 ceramics fabricated from the Si_3N_4–$Re_2Si_2O_7$ compositions.[12,19] In Si_3N_4 ceramics containing $Re_2Si_2O_7$ as a secondary phase, the formation of $Re_2Si_2O_7$ phase by oxidation leads to the depletion of Re^{+3} ions near surface, resulting in compositional gradient of Re^{+3} ions between the surface and bulk.[22] The compositional gradient of Re^{+3} ions is the driving force for the migration of Re^{+3} ions from the bulk to the surface since the $Re_2Si_2O_7$ phase is compatible with SiO_2.[7] Therefore, the compositional gradient of Re^{+3} ions as well as the incompatibility of Re–silicon oxynitride phases [$Y_{10}(SiO_4)_6N_2$, $Yb_4Si_2N_2O_7$, $Er_2Si_3N_4O_3$, and $La_{10}(SiO_4)_6N_2$] with SiO_2 act as the driving force for the oxidation of SNRe and result in the inferior oxidation resistance of the ceramics, compared to the Si_3N_4 from the Si_3N_4–$Re_2Si_2O_7$ compositions.

4 Summary

The oxidation behavior of four different Si_3N_4 ceramics fabricated from Si_3N_4–$Re_4Si_2N_2O_7$ (Re = Y, Yb, Er and La) compositions by hot-pressing was characterized and compared with that of Si_3N_4 ceramics fabricated from the Si_3N_4–$Re_2Si_2O_7$ compositions. XRD of the sintered specimens showed that silicon oxynitride phases [$Y_{10}(SiO_4)_6N_2$, $Yb_4Si_2N_2O_7$, $Er_2Si_3N_4O_3$, and $La_{10}(SiO_4)_6N_2$, respectively] were crystallized during cooling after sintering. All Si_3N_4 ceramics from Si_3N_4–$Re_4Si_2N_2O_7$ compositions showed parabolic weight gains with oxidation time at 1400°C for 192 h in air and the major oxidation products were SiO_2 and $Re_2Si_2O_7$. In both Si_3N_4–$Re_4Si_2N_2O_7$ and Si_3N_4–$Re_2Si_2O_7$ compositions, Er_2O_3 added to Si_3N_4 showed the best oxidation resistance among the compositions investigated, indicating that Er_2O_3 is a suitable sintering additive for the oxidation-resistant Si_3N_4 ceramics. The oxidation resistance of Si_3N_4 fabricated from Si_3N_4–$Re_4Si_2N_2O_7$ compositions was inferior to that of the Si_3N_4 from Si_3N_4–$Re_2Si_2O_7$ compositions, owing to the incompatibility of the Re–silicon oxynitride phases with SiO_2 in oxidizing conditions.

References

1. Isoke, J. L., Lange, F. F. and Diaz, E. S., Effect of selected impurities on the high temperature mechanical properties of hot-pressed silicon nitride. *J. Mater. Sci.*, 1976, **11**, 908–912.
2. Singhal, J. S. C., Thermodynamics and kinetics of oxidation of hot-pressed silicon nitride. *J. Mater. Sci.*, 1976, **11**, 500–509.
3. Cinibulk, M. K., Thomas, G. and Johnson, S. M., Fabrication and secondary-phase crystallization of rare-earth disilicate–silicon nitride ceramics. *J. Am. Ceram. Soc.*, 1992, **75**(8), 2037–2043.
4. Hwang, C. J., Fuller, S. M. and Beaman, D. R., Development of a high-performance Si_3N_4 material: using transient-liquid-phase and self-reinforcing technology. *Ceram. Eng. Sci. Proc.*, 1994, **15**, 685–693.
5. Thompson, D. P., New grain-boundary phases for nitrogen ceramics. In *Proceedings of the Material Research Society Symposium*, ed. I. W. Chen, P. F. Becher, M. Petzow, G. Petzow and T. S. Tien. Material Research Society, Pittsburgh, PA, 1993, pp. 79–92.
6. Hoffman, M. J. and Petzow, G., Microstructural design of Si_3N_4 based ceramics. In *Proceedings of the Material Research Society Symposium*, ed. I. W. Chen, P. F. Mitomo, M. Mitomo, G. Petzow and T. S. Tien. Material Research Society, Pittsburgh PA, 1993, pp. 3–14.
7. Lange, F. F., Singhal, S. C. and Kuznicki, R. C., Phase relationship and stability studies in the Si_3N_4–SiO_2–Y_2O_3 pseudoternary system. *J. Am. Ceram. Soc.*, 1977, **60**(5–6), 249–252.
8. Lange, F. F., Si_3N_4–CeO_2–SiO_2 materials: phase relationships and strength. *Am. Ceram. Soc. Bull.*, 1980, **59**(2), 239–249.
9. Sanders, W. A. and Mieskowski, D. M., Strength and microstructure of sintered Si_3N_4 with rare-earth oxide addition. *Am. Ceram. Soc. Bull.*, 1985, **64**(2), 304–309.
10. Hirosaki, N., Okada, A. and Matoba, K., Sintering of Si_3N_4 with the addition of rare-earth oxides. *J. Am. Ceram. Soc.*, 1988, **71**(3), 144–147.
11. Cinibulk, M. K., Thomas, G. and Johnson, S. M., Strength and creep behavior of rare-earth disilicate-silicon nitride ceramics. *J. Am. Ceram. Soc.*, 1992, **75**(8), 2050–2055.
12. Cinibulk, M. K. and Thomas, G., Oxidation behavior of rare-earth disilicate-silicon nitride ceramics. *J. Am. Ceram. Soc.*, 1992, **75**(8), 2044–2049.
13. Morgan, P. E. D., Lange, F. F., Clarke, D. R. and Davis, B. I., A new Si_3N_4 material: phase relations in the system Si–Sc–O–N and preliminary property studies. *J. Am. Ceram. Soc.*, 1981, **64**(4), 77–78.
14. Nishimura, T. and Mitomo, M., Phase relationship in the system Si_3N_4–SiO_2–Yb_2O_3. *J. Mat. Res.*, 1995, **10**(2), 240–242.
15. Nishimura, T. and Mitomo, M., High temperature strength of silicon nitride ceramics with ytterbium silicon oxynitride. *J. Mat. Res.*, 1997, **12**(1), 203–209.
16. Wills, R. R., Stewart, R. W., Cunningham, J. A. and Wimmer, J. M., The silicon lanthanide oxynitrides. *J. Mat. Sci.*, 1976, **11**, 749–759.
17. Montorsi, M. and Appendino, P., Silicon lanthanide oxynitrides of the $M_4Si_2O_7N_2$ type. *J. Less-Comm. Metals*, 1979, **68**, 193–197.
18. Wang, C. M., Pan, X., Hoffman, M. J., Cannon, R. M. and Ruhle, M., Grain boundary films in rare-earth-glass-based silicon nitride. *J. Am. Ceram. Soc.*, 1996, **79**(3), 788–792.
19. Choi, H. J., Lee, J. G. and Kim, Y.-W., High temperature strength and oxidation behaviour of hot-pressed silicon nitride-disilicate ceramics. *J. Mat. Sci.*, 1997, **32**, 1937–1942.
20. Choi, H. J., Lee, J. G. and Kim, Y.-W., High temperature strength and oxidation behaviour of $Er_2Si_2O_7$–Si_3N_4 ceramics. *J. Mat. Sci. Lett.*, 1996, **15**, 282–284.
21. Vetrano, J. S., Kleebe, H.-J., Hampp, E., Hoffman, M. J., Ruhle, M. and Cannon, R. M., Yb_2O_3-fluxed sintered silicon nitride. *J. Mat. Sci.*, 1993, **28**, 3529–3538.
22. Falk, L. K. L. and Engstrom, E. U., Elemental concentration profiles in an oxidized silicon nitride materials. *J. Am. Ceram. Soc.*, 1991, **74**(9), 2286–2292.